Acoustic Emission Signatures of Flow Boiling in a Microchannel Heat Sink

Stephen Pierson[1,2] Hari Pandey[1] Ben Xu[3]
Han Hu[1,2]

[1]Department of Mechanical Engineering, University of Arkansas, Fayetteville, AR 72701, USA
[2]University of Arkansas Power Group, University of Arkansas, Fayetteville, AR 72701, USA
[3]Department of Mechanical Engineering, University of Houston, Houston, TX 77204, USA

Abstract

Flow boiling in microchannel heat sinks is a promising route for next-generation electronics cooling, but its implementation is limited by interfacial instabilities, flow oscillations, vapor choking, and local dryout. Conventional diagnostics based on optical visualization, temperature, pressure, and flow-rate measurements are valuable, but they can be difficult to apply for real-time monitoring in compact or visually inaccessible cooling hardware. This work evaluates contact acoustic emission (AE) sensing as a nonintrusive diagnostic for identifying phase-change events and characterizing transient two-phase flow behavior in a microchannel heat sink. A synchronized multimodal facility was developed that combines contact AE sensing, airborne microphone measurements, thermofluidic measurements, and high-speed optical imaging under controlled heating conditions. Representative tests comparing a single-phase baseline at P = 2.2 W with a boiling case at P = 45.3 W show that boiling onset produces pronounced increases in AE amplitude and AE hit rate. The AE count-duration distribution also broadens during boiling and includes short-duration, high-count transients that are consistent with rapid interfacial motion and abrupt vapor-fraction changes. In contrast, microphone spectrograms show weaker separation between single-phase and two-phase conditions, indicating that solid-borne AE is more sensitive to confined boiling events under the tested conditions. These results establish a baseline framework for physics-informed acoustic diagnostics and machine-learning-assisted monitoring of two-phase thermal management systems.

Keywords: Acoustic emission, two-phase flows, microchannel heat sink, flow boiling, multimodal sensing, electronics cooling

1 Introduction

Flow boiling in microchannel heat sinks has emerged as a promising thermal-management strategy for next-generation electronics, electric propulsion systems, high-performance computing, and artificial-intelligence hardware because it can dissipate high heat fluxes within compact form factors. As chip and module power densities increase, conventional single-phase cooling approaches can require high pumping power or allow unacceptable temperature nonuniformity. Two-phase cooling uses latent heat transport and enhanced convection associated with bubble nucleation, growth, and evaporation to achieve higher heat-transfer coefficients than single-phase liquid cooling. Therefore, flow boiling has attracted sustained interest for power electronics, data centers, avionics, refrigeration systems, energy conversion systems, and microgravity thermal management [1–8]. However, practical implementation remains challenging because two-phase flows are unsteady and sensitive to operating condition, channel geometry, surface condition, and flow instability.

Two-phase flow instabilities arise from complex interactions among fluid inertia, vapor generation, evaporation momentum, surface tension, viscous stresses, pressure fluctuations, and buoyancy forces. These coupled phenomena produce a wide range of transient interfacial behaviors, including bubble nucleation, coalescence, vapor slug formation, annular flow transitions, intermittent dryout, pressure oscillations, flow reversal, and vapor choking. Flow instabilities can significantly degrade thermal performance by reducing the effective heat transfer coefficient, increasing pressure drop, inducing temperature oscillations, and triggering critical heat flux (CHF) conditions. The physical mechanisms governing these instabilities and CHF remain subjects of ongoing debate despite decades of investigation. Multiple mechanistic theories have been proposed to explain CHF during flow boiling, including boundary-layer separation [9–10], bubble crowding [11], sublayer dryout [12–15], and interfacial liftoff [16]. These theories emphasize different dominant mechanisms associated with vapor accumulation, liquid replenishment failure, and interfacial hydrodynamics near heated surfaces. To probe the instability mechanisms, extensive studies have examined flow boiling using high-speed optical imaging, infrared thermography, particle image velocimetry, and synchronized thermal-fluid measurements [17–26]. For example, Clark et al. [2] investigated pressure-drop oscillations and parallel-channel instabilities during microchannel flow boiling and demonstrated the strong coupling between hydraulic instability and CHF behavior. High-speed visualization studies by Chen and Garimella [18] provided detailed observations of bubble growth, confinement effects, and flow-regime transitions in silicon microchannel heat sinks. Similarly, Bigham et al. [17] investigated thin-film evaporation mechanisms on microstructured surfaces and demonstrated the role of microscale liquid-film dynamics in heat-transfer enhancement.

Although optical diagnostics have significantly advanced the understanding of two-phase flows, several important limitations remain. High-speed imaging requires direct optical access and is often difficult to implement in compact cooling systems, opaque geometries, or practical field environments. Furthermore, boiling flows exhibit substantial stochasticity due to the inherently transient and multiscale nature of bubble dynamics, making it challenging to define robust image-based signatures for flow-regime classification or anomaly detection. Large high-speed imaging datasets also require substantial storage and computational resources for processing. These limitations motivate the exploration of alternative nonintrusive sensing approaches capable of detecting transient boiling events and unstable flow behavior without relying exclusively on optical access. Acoustic emission (AE) sensing provides a complementary nonintrusive diagnostic for monitoring dynamic processes in complex thermal-fluid systems. AE signals are transient elastic waves generated by sudden energy-release events within materials or fluid-structure systems. AE sensing has been widely used in structural health monitoring, vibroacoustic system identification, damage detection, electrical-discharge diagnostics [27], and dynamic process monitoring [28–30]. In boiling systems, acoustic signals may originate from turbulence, rapid vapor expansion, bubble nucleation and collapse, interfacial oscillation, liquid-film rupture, and transient pressure fluctuations [31–32]. AE sensing has been increasingly explored for gas-liquid and vapor-liquid two-phase flow characterization. In gas-liquid systems, prior studies investigated flow-induced acoustic behavior for flow-pattern recognition, gas-volume-fraction estimation, leakage monitoring, and distributed sensing applications [33–37]. Xue et al. [33] examined the influence of gas bubbles on leakage acoustic wave propagation in gas-liquid systems and demonstrated strong sensitivity of acoustic signatures to bubble concentration and interfacial interactions. Zhao et al. [35, 37] investigated flow-induced acoustic characteristics in horizontal gas-liquid two-phase flows and demonstrated correlations between acoustic features and flow regimes. Distributed acoustic sensing approaches have also been applied for gas-phase velocity measurements and multiphase pipeline monitoring [34, 36]. Collectively, these studies demonstrate that acoustic signals contain rich information associated with interfacial structures and transient flow behavior. However, most of these investigations focused on non-phase-change systems and macroscale pipeline flows rather than confined boiling flows in microchannels.

In parallel, increasing attention has been directed toward acoustic diagnostics for boiling and phase-change heat transfer systems. Prior investigations demonstrated that boiling processes generate distinct acoustic signatures associated with bubble nucleation, vapor transport, and interfacial oscillations [38–47]. Lim et al. [42, 44] analyzed acoustic signal behavior during subcooled flow boiling and demonstrated the capability of acoustic measurements to identify boiling regimes nonintrusively. Barathula et al. [38] employed machine learning combined with boiling-induced vibration signals for heat-load prediction during flow boiling. More recently, Zhang et al. [39] demonstrated deep-learning-enabled identification of flow boiling regimes using acoustic measurements. Chen et al. [40–41] investigated the acoustic characteristics of flow boiling in helical tubes through both experimental and numerical approaches and demonstrated strong coupling between boiling dynamics and acoustic spectra. Several studies also explored the use of machine learning for predicting boiling heat flux, heat transfer coefficient, and boiling regimes from acoustic measurements [43, 48–50]. Recent work from the present research group has further demonstrated the potential of AE sensing for multiphase thermal-fluid diagnostics. Pandey et al. [31] reported a synchronized multimodal boiling dataset integrating acoustic sensing, optical imaging, and thermal measurements for boiling characterization under transient and steady-state conditions. Dunlap et al. [48] demonstrated nonintrusive heat-flux quantification during pool boiling using AE sensing, while subsequent studies developed machine-learning frameworks for boiling heat-flux prediction and transient heat-flux monitoring using hit-based AE features and temporal-spatial learning architectures [49–50]. Additional studies demonstrated acoustic sensing and unsupervised learning for phase-change flow characterization during condensation processes [46–47]. These studies indicate that acoustic measurements contain substantial latent information regarding interfacial dynamics and boiling intensity. However, most prior boiling-acoustic investigations focused on pool boiling, macroscale channels, or bulk spectral analysis. Relatively limited work has examined high-frequency contact AE sensing integrated with synchronized optical diagnostics for confined microchannel flow boiling. Despite the proven success of existing studies, there is still a fundamental lack of understanding regarding the physical origins of AE waveforms during boiling and the relationship between acoustic features and transient interfacial phenomena. Existing studies vary substantially in sensor type, frequency range, signal-processing method, and geometry, which limits cross-study comparison and slows the development of generalized acoustic diagnostic frameworks. The distinction between airborne acoustic measurements from microphones and solid-borne transient signals from contact AE sensors also remains insufficiently investigated for confined boiling systems. This distinction is practically important because electronics-cooling hardware often contains compact, opaque, or embedded flow paths where optical access is unavailable and real-time instability monitoring is needed.

To address these challenges, this work investigates contact AE sensing for detecting and characterizing two-phase flow behavior in a microchannel heat sink. A synchronized multimodal platform integrating AE sensing, microphone measurements, thermofluidic sensing, and high-speed optical imaging is developed for flow boiling experiments under controlled heating conditions. The study compares acoustic behavior between single-phase and two-phase flow conditions and evaluates AE amplitude, hit rate, waveform duration, counts, and spectrogram characteristics during boiling onset and vapor transport. Particular emphasis is placed on distinguishing the capabilities of contact-based AE sensing and airborne microphone measurements for detecting transient boiling events in confined microchannels. The presented framework establishes a foundation for physics-informed acoustic diagnostics, machine-learning-assisted boiling-regime classification, and real-time monitoring of advanced two-phase thermal-management systems. The specific contributions of this paper are threefold. First, a microchannel flow-boiling facility is integrated with synchronized contact AE, microphone, thermal-fluid, and optical measurements. Second, representative single-phase and two-phase cases are used to identify AE features that respond strongly to boiling onset and vapor transport. Third, contact AE and airborne microphone measurements are compared to clarify why solid-borne acoustic sensing is advantageous for detecting confined phase-change events under the present test conditions.

2 Methodology

Figure 1a illustrates the in-house flow loop developed for single-phase and two-phase cooling experiments, with preliminary calibration reported in [51]. The inlet and outlet fluid temperatures were measured using epoxy-coated 3950 NTC thermistors connected in voltage-divider circuits with fixed 10 kΩ resistors. Differential pressure across the heat sink was measured using an Omega Engineering PX2300-10DI differential-pressure transducer connected through 1/16-inch tubing. A Koolance PMP-500 pump driven by an external power supply controlled the liquid flow rate, while an Omega BV1000TRN025B turbine flow meter measured the instantaneous flow rate. Fluid temperature conditioning was achieved using a jacketed reaction vessel coupled to a Thermo Scientific Polar ACCEL 500 chiller. An inline preheater controlled by an INKBIRD PID controller maintained the desired inlet temperature. Heating power was supplied using a ceramic heating plate attached beneath the heat sink with thermally conductive paste. The integrated K-type thermocouple within the heater monitored the base temperature of the heat sink. Temperature and flow-rate data were collected at 1 Hz with an Arduino Uno, converted to engineering values, and exported to text files for post-processing.

Figure 1b shows the test section integrated with optical and acoustic sensing. A straight microchannel heat sink with channel depth D = 500 µm, width W = 500 µm, and spacing S = 500 µm was used for all tests reported in this study. A Phantom VEO 710L high-speed camera with a Nikon AF-S Micro-NIKKOR 60 mm f/2.8G ED lens captured the two-phase flow behavior at 1,000 frames per second. A MISTRAS R3a contact AE sensor was attached to the side wall of the test section using a magnetic hold-down fixture. The AE sensor was connected to a MISTRAS USB AE Node, and data were acquired using AEWin software. The saved source files (.DTA) were converted into waveform and hit data for analysis. A Behringer ECM8000 condenser microphone was positioned near the test section and connected to a Behringer U-PHORIA UMC404HD data-acquisition interface powered by a Neewer NW-100 supply. The microphone signal was recorded through LabVIEW to compare airborne acoustic response with contact AE response.

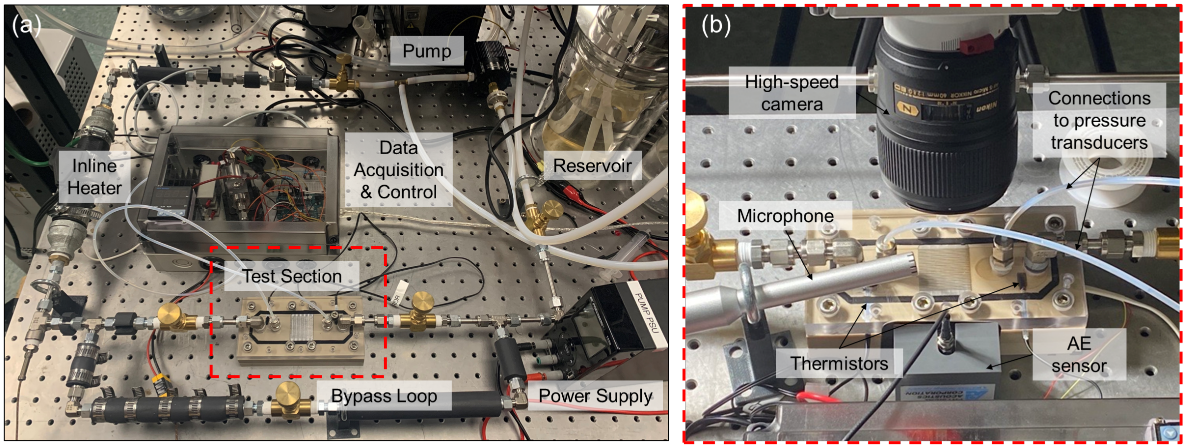

Figure 1: Photographs of (a) the flow loop for two-phase flow testing and (b) the test section with high-speed imaging and acoustic sensing using an AE sensor and a microphone.

Figure 2 illustrates the threshold-based hit analysis used for the AE data using a representative waveform from single-phase flow. The AE amplitude is defined as the maximum signal magnitude during a transient event, and the rise time is the interval between the first threshold crossing and the peak amplitude. The signal duration is the total time interval over which the waveform remains above the threshold, while AE counts represent the number of threshold crossings within the event. Counts therefore provide a compact measure of waveform oscillation and complexity. These hit-based parameters are widely used in structural health monitoring and are useful here because they reduce high-rate transient waveforms into interpretable event-level quantities that can be compared with flow state and optical observations.

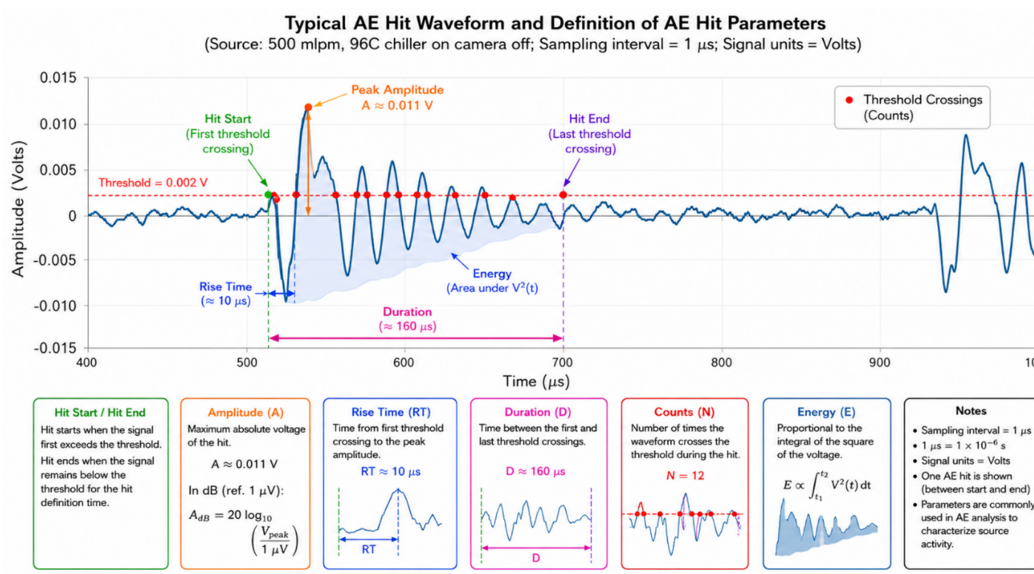

Figure 2: Illustration of AE hit parameters using a representative AE waveform during single-phase flows.

The present analysis is intentionally framed as a feasibility study rather than a complete flow-regime classifier. Optical images are used to identify whether the test remains single phase or contains vapor generation, while AE features are used to quantify the corresponding acoustic activity. Because AE amplitude depends on sensor coupling, propagation path, and threshold settings, the comparisons in this paper emphasize relative differences between tests conducted on the same facility rather than universal amplitude thresholds. Future datasets should report repeated trials, uncertainty bounds, and sensor-position sensitivity before model parameters are generalized across heat-sink designs.

3 Results and Discussion

Figure 3 compares representative AE amplitude histories for single-phase and two-phase flow in the microchannels. At a heater power of P = 2.2 W, the flow remains single phase during the test, and the AE amplitude stays near the background level with only small fluctuations. At P = 45.3 W, the flow initially remains liquid, but bubbles nucleate in the channels as heat accumulates and the wall superheat increases. After vapor generation begins, the AE response shows substantially larger transient amplitudes than the single-phase baseline. This contrast indicates that contact AE sensing is sensitive to the onset of phase change and to the accompanying interfacial dynamics in the confined channels. Physically, the stronger AE response is consistent with rapid bubble growth, vapor transport, local pressure disturbances, and fluid-structure excitation caused by intermittent two-phase motion.

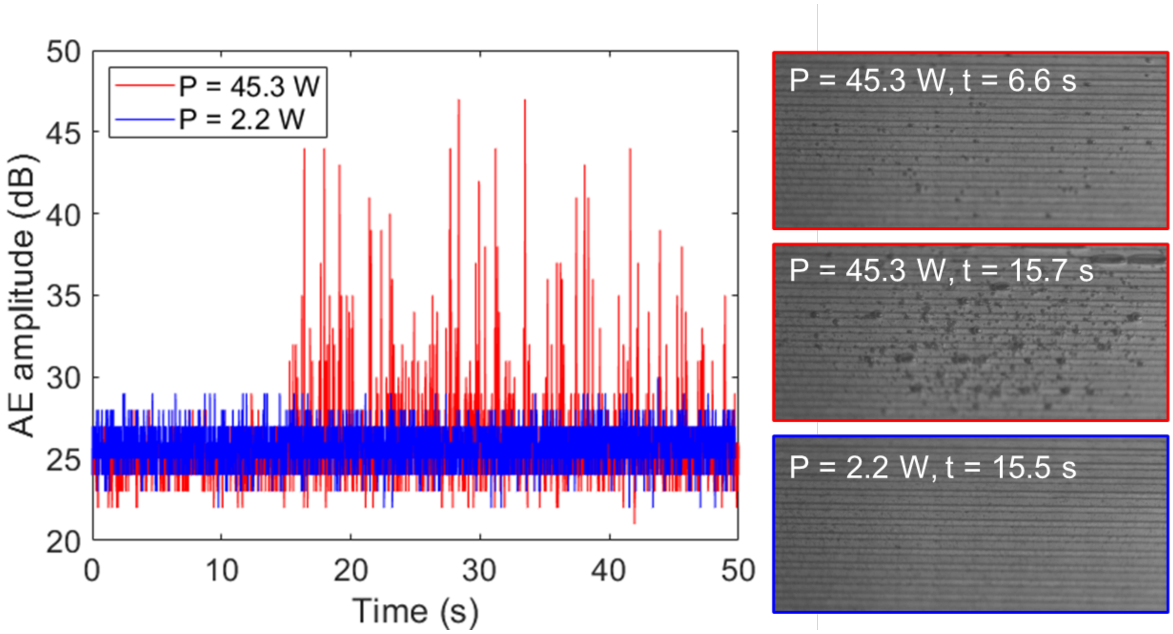

Figure 3: Comparison of the AE amplitude versus time between the single-phase flow test (P = 2.2 W) and the two-phase flow test (P = 45.3 W). The optical images with blue and red borders represent the single-phase flow test and the two-phase flow test, respectively.

Figure 4 compares AE counts versus signal duration for the single-phase and two-phase flow conditions. In both cases, AE counts generally increase with waveform duration because longer events contain more oscillatory cycles crossing the threshold level. However, the two-phase condition exhibits a broader distribution of AE events, including short-duration, high-count waveforms associated with rapid transient dynamics. These events are consistent with sudden interfacial motion, vapor slug acceleration, or abrupt vapor-fraction fluctuations rather than the smoother hydrodynamic background expected during single-phase flow. Compared with the compact single-phase distribution, the broader boiling distribution indicates a more intermittent acoustic source field. The result suggests that joint feature distributions, rather than amplitude alone, may provide a useful basis for future flow-regime classification and anomaly detection.

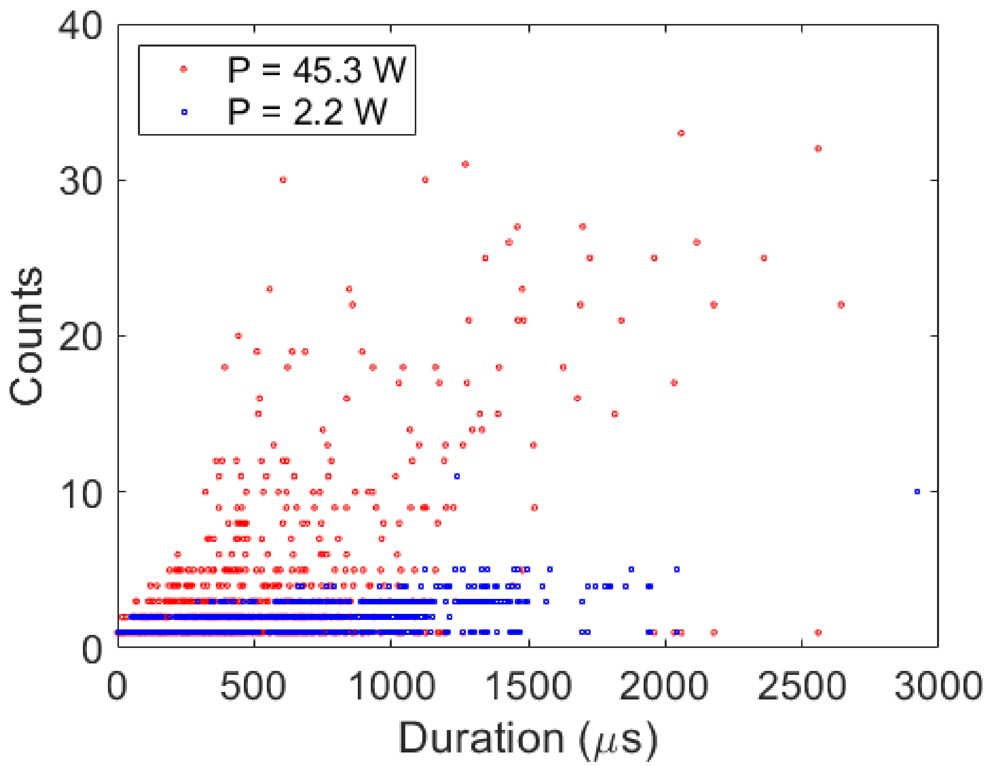

Figure 4: Comparison between the single-phase flow test (P = 2.2 W) and the two-phase flow test (P = 45.3 W) for AE counts versus duration.

Figure 5 presents the AE hit rate and AE amplitude evolution during the two-phase flow experiment. The onset of boiling corresponds to a sharp increase in both AE amplitude and hit frequency. As vapor generation intensifies, repeated transient acoustic bursts are observed throughout the experiment. The increase in AE hit rate reflects the increasing frequency of threshold-crossing interfacial events within the microchannels. Because AE hits represent discrete transient events rather than time-averaged temperature or pressure measurements, the hit rate can serve as a real-time indicator of boiling activity intensity. These observations suggest that AE hit statistics may be useful for detecting unstable or high-activity operating conditions in compact cooling systems.

Microphone data were also analyzed to evaluate whether airborne sound provides comparable sensitivity to flow boiling. Figure 6 compares microphone spectrograms obtained during the single-phase and two-phase conditions. Unlike the contact AE measurements, the microphone spectrograms do not show a clear regime-dependent pattern under the tested conditions. This difference is likely caused by weak airborne acoustic radiation from the confined phase-change events and by attenuation across the fluid-solid-air transmission path. High-frequency components generated by bubble nucleation, rapid vapor expansion, or interfacial impact are expected to be especially sensitive to this transmission loss. The comparison therefore indicates that contact AE sensing is better suited than airborne microphone sensing for detecting the solid-borne transient signatures produced by microchannel flow boiling in this facility.

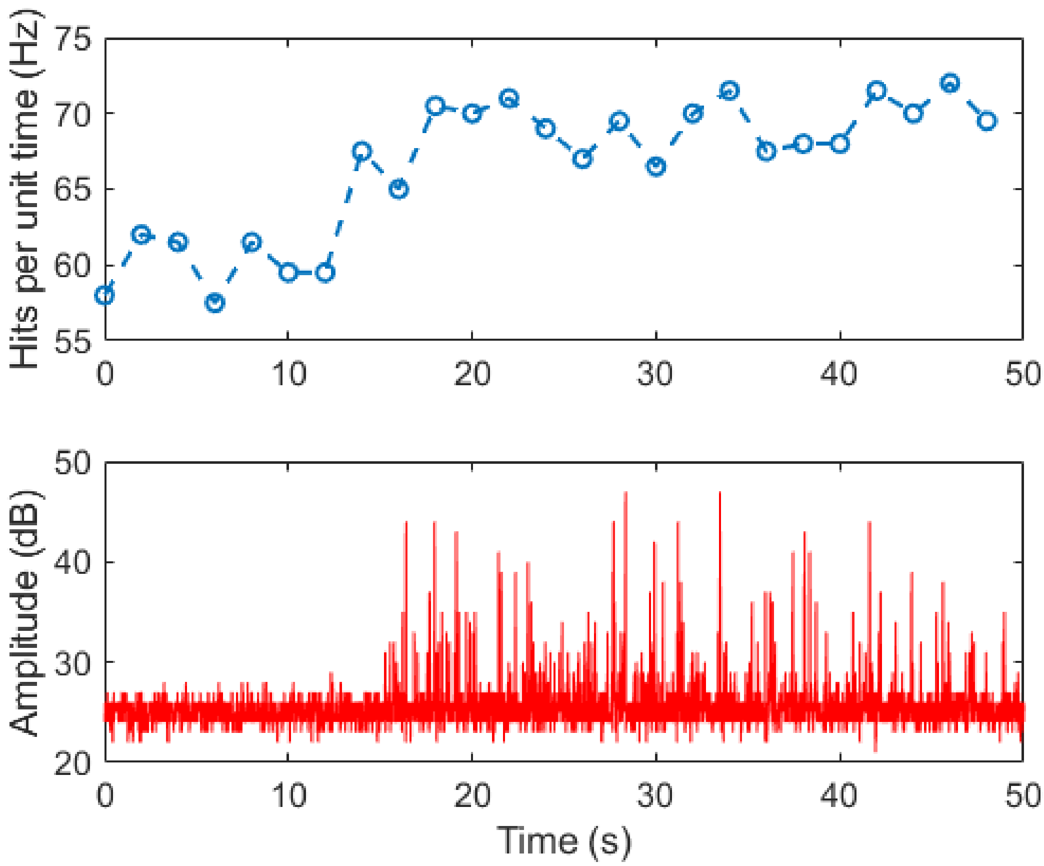

Figure 5: AE hit per unit time and AE amplitude versus time for the two-phase flow test.

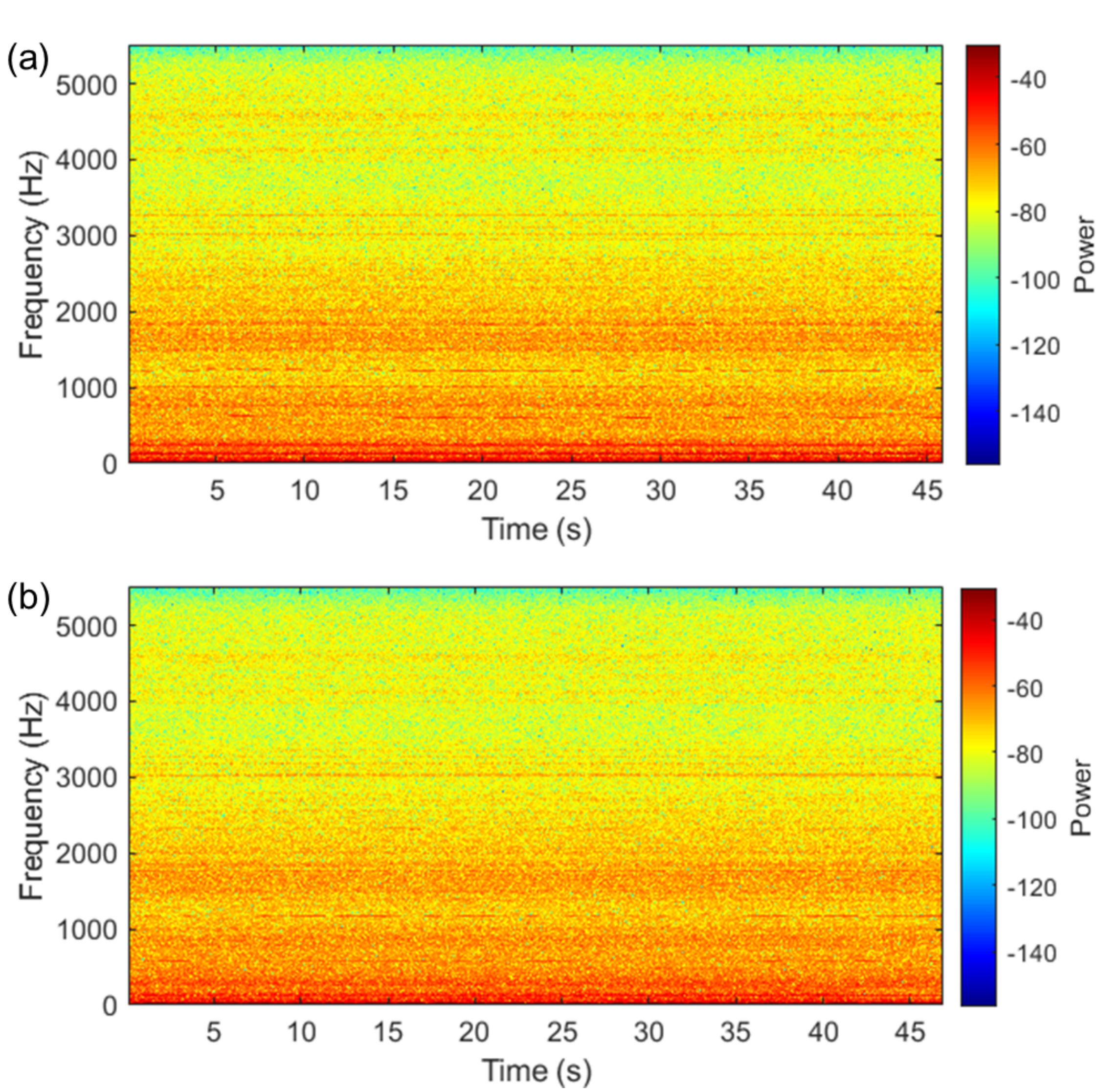

Figure 6: Comparison of the spectrogram of the microphone data between (a) the single-phase flow test (P = 2.2 W) and (b) the two-phase flow test (P = 45.3 W).

The results should be interpreted with several limitations in mind. The present dataset compares representative single-phase and boiling cases rather than a fully replicated design of experiments over mass flux, inlet subcooling, heat flux, and channel geometry. The AE source mechanisms are inferred from synchronized optical observations and thermal-fluid state rather than isolated source calibration. In addition, the AE threshold, sensor coupling, and propagation path influence the absolute hit statistics. These limitations do not weaken the main feasibility result, but they motivate future experiments that include repeated trials, uncertainty quantification, controlled boiling-regime labels, and sensor-placement studies.

4 Conclusion

This work demonstrates the use of contact acoustic emission sensing for detecting and characterizing two-phase flow behavior in a microchannel heat sink. A synchronized multimodal platform integrating AE sensing, microphone measurements, thermal sensing, hydraulic measurements, and high-speed optical imaging was developed for flow boiling experiments. Representative tests showed clear differences between single-phase and two-phase conditions in AE amplitude, hit rate, waveform duration, and count-duration distributions. Boiling produced stronger and more frequent transient AE activity, consistent with bubble nucleation, vapor transport, and intermittent interfacial motion within the microchannels. Airborne microphone measurements showed weaker separation between the same operating states, indicating that solid-borne AE sensing is more sensitive to confined boiling events under the tested conditions. The results support AE sensing as a promising nonintrusive diagnostic for real-time monitoring of boiling flows and interfacial instabilities in compact thermal-management systems. Future work will focus on replicated operating maps, uncertainty quantification, synchronized analysis with infrared thermography and high-speed imaging, and machine-learning-assisted classification of boiling regimes and anomalous flow events.

Acknowledgments

This work was supported by the National Science Foundation under Grant No. 2323022 and Grant No. 2431969.

Data Availability

Data is publicly available through Dryad under a CC0 public domain dedication at `https://doi.org/10.5061/dryad.kwh7orzm3`.

References

[1] M. H. Matin and S. Moghaddam, "Prediction of regime transition in two phase flow microchannels based on ultrathin liquid film interfacial instability," InterSociety Conference on Thermal and Thermomechanical Phenomena in Electronic Systems, ITHERM, vol. 2019-May, pp. 1190-1196, 2019, doi: 10.1109/ITHERM.2019.8757264.

[2] M. D. Clark, J. A. Weibel, and S. V Garimella, "Impact of pressure drop oscillations and parallel channel instabilities on microchannel flow boiling and critical heat flux," International Journal of Multiphase Flow, vol. 161, no. June 2022, p. 104380, 2023, doi: 10.1016/j.ijmultiphaseflow.2023.104380.

[3] S. Bhavnani, V. Narayanan, W. Qu, M. Jensen, S. Kandlikar, J. Kim, and J. Thome, "Boiling augmentation with Micro/Nanostructured surfaces: Current status and research outlook," Nanoscale and Microscale Thermophysical Engineering, vol. 18, no. 3, pp. 197-222, 2014, doi: 10.1080/15567265.2014.923074.

[4] J. F. Klausner, B. T. Chao, and S. L. Soo, "An improved method for simultaneous determination of frictional pressure drop and vapor volume fraction in vertical flow boiling," Exp. Therm. Fluid Sci., vol. 3, no. 4, pp. 404-415, 1990, doi: 10.1016/0894-1777(90)90039-A.

[5] C. N. Huang and C. R. Kharangate, "A new mechanistic model for predicting flow boiling critical heat flux based on hydrodynamic instabilities," Int. J. Heat Mass Transf., vol. 138, pp. 1295-1309, 2019, doi: 10.1016/j.ijheatmasstransfer.2019.04.103.

[6] M. Kim and M. Kaviany, "Flow-boiling canopy wick for extreme heat transfer," Int. J. Heat Mass Transf., vol. 117, pp. 1158-1168, 2018, doi: 10.1016/j.ijheatmasstransfer.2017.10.079.

[7] A. K. Vutha, S. R. Rao, F. Houshmand, and Y. Peles, “Active control of flow boiling oscillation amplitude and frequency using a transverse jet in crossflow,” Appl. Phys. Lett., vol. 108, no. 13, 2016, doi: 10.1063/1.4945334.

[8] R. Naik and A. Narain, “Steady and unsteady simulations for annular internal condensing flows, part II: Instability and flow regime transitions,” Numerical Heat Transfer, Part B: Fundamentals, vol. 69, no. 6, pp. 495-510, 2016, doi: 10.1080/10407790.2016.1138804.

[9] W. D. and M. D. W. HEBEL, “A Contribution to the Hydrodynamics of Boiling Crisis in a Forced Flow of Water,” Nuclear Engineering and Design, vol. 64, pp. 433-445, 1981.

[10] J. Weisman and B. S. Pei, “Prevision du flux thermique critique dans un ecoulement avec ebullition a faible qualite,” Int. J. Heat Mass Transf., vol. 26, no. 10, pp. 1463-1477, 1983, doi: 10.1016/S0017-9310(83)80047-7.

[11] C. H. Lee and I. Mudawwar, “A mechanistic critical heat flux model for subcooled flow boiling based on local bulk flow conditions,” International Journal of Multiphase Flow, vol. 14, no. 6, pp. 711-728, 1988, doi: 10.1016/0301-9322(88)90070-5.

[12] J. E. Galloway and I. Mudawar, “CHF mechanism in flow boiling from a short heated wall-II. Theoretical CHF model,” Int. J. Heat Mass Transf., vol. 36, no. 10, pp. 2527-2540, 1993, doi: 10.1016/S0017-9310(05)80191-7.

[13] J. E. Galloway and I. Mudawar, “CHF mechanism in flow boiling from a short heated wall-I. Examination of near-wall conditions with the aid of photomicrography and high-speed video imaging,” Int. J. Heat Mass Transf., vol. 36, no. 10, pp. 2511-2526, 1993, doi: 10.1016/S0017-9310(05)80190-5.

[14] J. C. Sturgis and I. Mudawar, “Critical heat flux in a long, rectangular channel subjected to one-sided heating-I. flow visualization,” Int. J. Heat Mass Transf., vol. 42, no. 10, pp. 1835-1847, 1999, doi: 10.1016/S0017-9310(98)00274-9.

[15] J. C. Sturgis and I. Mudawar, “Critical heat flux in a long, rectangular channel subjected to one-sided heating-II. Analysis of critical heat flux data,” Int. J. Heat Mass Transf., vol. 42, no. 10, pp. 1849-1862, 1999, doi: 10.1016/S0017-9310(98)00275-0.

[16] M. Cumo, “The influence of inclination on CHF in steam generators channels,” RT/ING, no. 78, 1978.

[17] S. Bigham, A. Fazeli, and S. Moghaddam, “Physics of microstructures enhancement of thin film evaporation heat transfer in microchannels flow boiling,” Sci. Rep., vol. 7, no. February, pp. 1-11, 2017, doi: 10.1038/srep44745.

[18] T. Chen and S. v. Garimella, “Measurements and high-speed visualizations of flow boiling of a dielectric fluid in a silicon microchannel heat sink,” International Journal of Multiphase Flow, vol. 32, no. 8, pp. 957-971, 2006, doi: 10.1016/j.ijmultiphaseflow.2006.03.002.

[19] S. v. Garimella, A. S. Fleischer, J. Y. Murthy, A. Keshavarzi, R. Prasher, C. Patel, S. H. Bhavnani, R. Venkatasubramanian, R. Mahajan, Y. Joshi, B. Sammakia, B. A. Myers, L. Chorosinski, M. Baelmans, P. Sathyamurthy, and P. E. Raad, “Thermal challenges in next-generation electronic systems,” IEEE Transactions on Components and Packaging Technologies, vol. 31, no. 4, pp. 801-815, 2008, doi: 10.1109/TCAPT.2008.2001197.

[20] J. Gess, S. Bhavnani, and R. Wayne Johnson, "Single-and Two-Phase Particle Image Velocimetry Characterization of Fluid Flow Within a Liquid Immersion Cooled Electronics Module," Journal of Electronic Packaging, Transactions of the ASME, vol. 138, no. 4, 2016, doi: 10.1115/1.4034854.

[21] C. R. Kharangate, I. Mudawar, and M. M. Hasan, "Photographic study and modeling of critical heat flux in horizontal flow boiling with inlet vapor void," Int. J. Heat Mass Transf., vol. 55, no. 15-16, pp. 4154-4168, 2012, doi: 10.1016/j.ijheatmasstransfer.2012.03.057.

[22] J. Y. Lee, M. H. Kim, M. Kaviany, and S. Y. Son, "Bubble nucleation in microchannel flow boiling using single artificial cavity," Int. J. Heat Mass Transf., vol. 54, no. 25-26, pp. 5139-5148, 2011, doi: 10.1016/j.ijheatmasstransfer.2011.08.042.

[23] A. Parahovnik, U. Manda, and Y. Peles, "Heat transfer mode shift to adiabatic thermalization in near-critical carbon dioxide with flow boiling in a microchannel," Int. J. Heat Mass Transf., vol. 188, p. 122629, 2022, doi: 10.1016/j.ijheatmasstransfer.2022.122629.

[24] M. T. Lebon, C. F. Hammer, and J. Kim, "Gravity effects on subcooled flow boiling heat transfer," Int. J. Heat Mass Transf., vol. 128, pp. 700-714, 2019, doi: 10.1016/j.ijheatmasstransfer.2018.09.011.

[25] F. Cui, F. Hong, C. Li, and P. Cheng, "International Journal of Heat and Mass Transfer Two-phase flow instability in distributed jet array impingement boiling on pin-fin structured surface and its affecting factors," Int. J. Heat Mass Transf., vol. 143, p. 118495, 2019, doi: 10.1016/j.ijheatmasstransfer.2019.118495.

[26] M. Alwazzan, K. Egab, B. Peng, J. Khan, and C. li, "Condensation on hybrid-patterned copper tubes (II): Visualization study of droplet dynamics," Int. J. Heat Mass Transf., vol. 112, pp. 950-958, 2017, doi: 10.1016/j.ijheatmasstransfer.2017.05.040.

[27] J. Frankhouse, C. Li, and H. Hu, "Acoustic Characterization of Integrated Circuits During Operation," J. Electron. Packag., pp. 1-25, Jun. 2024, doi: 10.1115/1.4065649.

[28] D. F. Hesser, S. Mostafavi, G. K. Kocur, and B. Markert, "Identification of acoustic emission sources for structural health monitoring applications based on convolutional neural networks and deep transfer learning," Neurocomputing, vol. 453, pp. 1-12, 2021, doi: 10.1016/j.neucom.2021.04.108.

[29] O. A. Ibrahim, S. Sciancalepore, and R. di Pietro, "Noise2Weight: On detecting payload weight from drones acoustic emissions," Future Generation Computer Systems, vol. 134, pp. 319-333, 2022, doi: 10.1016/j.future.2022.03.041.

[30] C. R. Farrar and G. H. James, "System identification from ambient vibration measurements on a bridge," J. Sound Vib., vol. 205, no. 1, pp. 1-18, 1997, doi: 10.1006/jsvi.1997.0977.

[31] H. Pandey, C. Li, and H. Hu, "Multimodal boiling dataset with synchronized acoustic, optical, and thermal measurements under steady-state and transient heat loads," Date Brief, vol. 55, p. 110582, 2024, doi: 10.7910/DVN/6GLGC6.

[32] H. Pandey, H. Mehrabi, A. Williams, C. Mira-Hernandez, R. H. Coridan, and H. Hu, "Acoustic sensing for investigating critical heat flux enhancement during pool boiling on electrodeposited copper foams," Appl. Therm. Eng., vol. 236, p. 121807, 2024, doi: 10.1016/j.applthermaleng.2023.121807.

[33] Y. Xue, L. Yue, R. Ding, S. Zhu, C. Liu, and Y. Li, "Influencing mechanisms of gas bubbles on propagation characteristics of leakage acoustic waves in gas-liquid two-phase flow," Ocean Engineering, vol. 273, no. January, p. 114027, 2023, doi: 10.1016/j.oceaneng.2023.114027.

[34] G. Heim Weber, E. N. Dos Santos, D. F. Gomes, A. L. B. Santana, J. C. C. Da Silva, C. Martelli, D. R. Pipa, R. E. M. Morales, S. T. De Camargo Junior, M. F. Da Silva Junior, and M. J. Da Silva, "Measurement of Gas-Phase Velocities in Two-Phase Flow Using Distributed Acoustic Sensing," IEEE Sens. J., vol. 23, no. 4, pp. 3597-3608, 2023, doi: 10.1109/JSEN.2022.3232269.

[35] N. Zhao, G. Zhu, J. Feng, X. Luo, and J. Song, "Experimental investigation on characteristics of flow-induced acoustics in horizontal gas-liquid two-phase flow," International Journal of Multiphase Flow, vol. 192, no. February, p. 105378, 2025, doi: 10.1016/j.ijmultiphaseflow.2025.105378.

[36] K. peng Zhang, H. chu Ku, X. ge He, H. long Lu, M. Zhang, and C. bin Guo, "Measurement of gas and liquid flow rates in two-phase pipe flows with distributed acoustic sensing," Measurement (Lond)., vol. 250, no. February, p. 117137, 2025, doi: 10.1016/j.measurement.2025.117137.

[37] N. N. Zhao, J. J. Feng, G. J. Zhu, G. K. Wu, and X. Q. Luo, "Characterization of the horizontal gas-liquid two-phase flow patterns using acoustic measurement techniques," Physics of Fluids, vol. 37, no. 1, 2025, doi: 10.1063/5.0250150.

[38] S. Barathula, R. Kandasamy, P. J. Y. Fok, T. N. Wong, K. C. Leong, and K. Srinivasan, "Heat load prediction in flow boiling using boiling-induced vibrations aided with machine learning," Int. J. Heat Mass Transf., vol. 232, no. January, p. 125890, 2024, doi: 10.1016/j.ijheatmasstransfer.2024.125890

[39] K. Zhang, J. Yang, C. Huang, and X. Huai, "Nonintrusive identification of boiling regimes enabled by deep learning based on flow boiling acoustics," Int. J. Heat Mass Transf., vol. 236, no. P1, p. 126290, 2025, doi: 10.1016/j.ijheatmasstransfer.2024.126290.

[40] C. G. Chen, X. Y. Hao, Y. P. Mou, X. Bin Li, H. N. Zhang, and F. C. Li, "Experimental investigation on flow boiling induced acoustic characteristics in a helical tube," International Communications in Heat and Mass Transfer, vol. 172, no. P4, p. 110514, 2026, doi: 10.1016/j.icheatmasstransfer.2026.110514.

[41] C. G. Chen, X. Bin Li, H. N. Zhang, and F. C. Li, "Numerical study on acoustic characteristics of flow boiling in a helical tube," Appl. Therm. Eng., vol. 247, no. March, p. 123090, 2024, doi: 10.1016/j.applthermaleng.2024.123090.

[42] D. Y. Lim, J. Y. Kim, and I. C. Bang, "Subcooled Flow Boiling with Analysis of Acoustic Signal Behavior," 2021, [Online]. Available: Do Yeong.

[43] D. Lim, Y. Liu, and I. C. Bang, "Predicting boiling heat flux, heat transfer coefficient, and regimes Non-intrusively using external acoustics and deep learning," Sci. Rep., vol. 15, no. 1, pp. 1-18, 2025, doi: 10.1038/s41598-025-08183-z.

[44] D. Y. Lim, J. Y. Kim, D. H. Lee, K. M. Kim, and I. C. Bang, "Identifying Heat Transfer Regimes by Acoustic Analysis in Pool and Flow Boiling," pp. 9-11, 2020.

[45] P. Huang, J. H. Seong, J. M. Castro-aguilar, and E. M. O. Brien, "A non-intrusive framework using acoustic signals and deep learning for boiling diagnostics in visual-limited environments IN IN," 2026.

[46] L. Yan, D. Wallen, A. Allam, H. Hu, K. Bellur, and Y. Sun, "Slug flow condensation identification with acoustic signatures," Int. J. Heat Mass Transf., vol. 256, no. P3, p. 128144, 2026, doi: 10.1016/j.ijheatmasstransfer.2025.128144.

[47] D. Wallen, L. Yan, C. Dunlap, C. Li, H. Hu, and Y. Sun, "Unsupervised machine learning framework for non-destructive acoustic emission sensing of flow condensation," AI Thermal Fluids, vol. 2-3, no. April, p. 100010, 2025, doi: 10.1016/j.aitf.2025.100010.

[48] C. Dunlap, H. Pandey, E. Weems, and H. Hu, “Nonintrusive heat flux quantification using acoustic emissions during pool boiling,” Appl. Therm. Eng., vol. 228, no. December 2022, p. 120558, 2023, doi: 10.1016/j.applthermaleng.2023.120558.

[49] C. Dunlap, C. Li, H. Pandey, and H. Hu, “Hit2flux: A machine learning framework for boiling heat flux prediction using hit-based acoustic emission sensing,” AI Thermal Fluids, vol. 1, no. February, p. 100002, 2025, doi: 10.1016/j.aitf.2025.100002.

[50] C. Dunlap, C. Li, H. Pandey, Y. Sun, and H. Hu, “A Temporal-Spatial Framework for Efficient Heat Flux Monitoring of Transient Boiling,” IEEE Trans. Instrum. Meas., vol. 73, pp. 1-12, 2024, doi: 10.1109/TIM.2024.3460944.

[51] S. Pierson, N. Nawar, and H. Hu, “Comparing the Thermal Performance of Microchannel Heat Sinks Produced by CNC Milling Versus Power Bed Fusion,” 2023.